Impact of the Agulhas Current on Southern Africa Precipitation: A Modeling Study

ARIELLE STELA N. IMBOL NKWINKWA,[a,b,c] MATHIEU ROUAULT,[b,c] NOEL KEENLYSIDE,[d,e] AND SHUNYA KOSEKI[d]

[a] *GEOMAR Helmholtz Centre for Ocean Research Kiel, Kiel, Germany*
[b] *Department of Oceanography, University of Cape Town, Cape Town, South Africa*
[c] *Nansen-Tutu Centre for Marine Environmental Research, University of Cape Town, Cape Town, South Africa*
[d] *Geophysical Institute, University of Bergen/Bjerknes Centre for Climate Research, Bergen, Norway*
[e] *Nansen Environmental and Remote Sensing Center, Bjerknes Centre for Climate Research, Bergen, Norway*

(Manuscript received 7 August 2020, in final form 14 September 2021)

ABSTRACT: The Agulhas Current (AC) creates a sharp temperature gradient with the surrounding ocean, leading to a large turbulent flux of moisture from ocean to atmosphere. We use two simulations of the Weather Research and Forecasting (WRF) Model to show the seasonal impact of the warm core of the AC on southern Africa precipitation. In one simulation the sea surface temperature (SST) of the AC is similar to satellite observations, while the second uses satellite SST observations spatially smoothed to reduce the temperature of the core of the AC by ~1.5°C. We show that decreasing the SST of the AC reduces the precipitation of the wettest seasons (austral summer and autumn) inland. Over the ocean, reducing the SST reduces precipitation, low-level wind convergence, SST, and SLP Laplacians above the AC in all seasons, consistent with the pressure adjustment mechanism. Moreover, winter precipitation above the AC may also be related to increased latent flux. In summer and autumn, the AC SST reduction is also associated with decreased precipitation farther inland (more than 1.5 mm day^{-1}), caused by an atmospheric circulation that decreases the horizontal moisture flux from the AC to South Africa. The reduction is also associated with higher geopotential height extending from the surface east and over the AC to the midtroposphere over southeastern Africa. The westward tilted geopotential height is consistent with the linear response to shallow diabatic heating in midlatitudes. An identical mechanism occurs in spring but is weaker. Winter rainfall response is confined above the AC.

KEYWORDS: Atmosphere-ocean interaction; Boundary currents; Precipitation; Regional models

1. Introduction

Ocean–atmosphere interaction is a key element of southern Africa weather and climate. During the last decades much has been learned about how the oceans can influence the climate of southern Africa (Reason 2017; Monerie et al. 2018). This offers predictability at the seasonal scale and possibly at the decadal scale (Dieppois et al. 2016). This also indicates that the future climate of southern Africa will be influenced by the future state of the oceans under natural and anthropogenic forcing.

Southern Africa has a subtropical climate; it is relatively dry and is affected by temperate and tropical weather systems (Reason 2017). The region is under the influence of the South Atlantic and south Indian Ocean high pressure systems. There are two main climatic regimes: the southwest region gets most of its rainfall in austral winter (June–August), whereas the rest of southern Africa gets most of its rainfall in austral summer (Reason 2017). However, the south coast gets rainfall all year long (Engelbrecht et al. 2015; Engelbrecht and Landman 2016). Cold fronts (Favre et al. 2013) produce most of the rainfall in the southwest in winter whereas cutoff lows can occur at all seasons with a preference for spring (Singleton and Reason 2007; Favre et al. 2013).

In summer most rainfall is of convective origin and is influenced by large-scale dynamics (Reason 2017). Besides cutoff lows, rainfall is mainly produced by mesoscale convective complexes (Blamey and Reason 2013), tropical temperate troughs (Vigaud et al. 2012; Hart et al. 2013; Macron et al. 2014), and occasionally by tropical cyclones or tropical low pressure systems associated with easterly waves (Malherbe et al. 2012). The Botswana high (Driver and Reason 2017; Reason 2017) and the Angola low (Crétat et al. 2019) as well as the Mozambique Channel (Barimalala et al. 2018), the southwest Indian Ocean (Reason and Mulenga 1999), and the Angola Current (Desbiolles et al. 2018, 2020) also have an impact on seasonal rainfall variability. In addition, South African summer rainfall has a clear diurnal cycle of precipitation (e.g., Rouault et al. 2013; Pohl et al. 2014; Koseki et al. 2018). The standardized amplitudes, indicative of the strength of the diurnal cycle across a region, are strongest over the interior and along the east coast of South Africa with up to 70% explained variance of hourly rainfall associated with the diurnal cycle (Rouault et al. 2013). The time of maximum precipitation is from late afternoon to early evening in the interior and from midnight to early morning along the Agulhas Current (Rouault et al. 2013; Koseki et al. 2018).

In summer, a heat low is found over the interior of the southern African continent. This low tends to increase precipitation by

Supplemental information related to this paper is available at the Journals Online website: https://doi.org/10.1175/JCLI-D-20-0627.s1.

Corresponding author: Arielle Stela Imbol Nkwinkwa Njouodo, aimbol@geomar.de

DOI: 10.1175/JCLI-D-20-0627.1

weakening the subsidence associated with high pressure systems (Tyson and Preston-White 2000). Moreover, most of the interior lies on an elevated plateau, and the orography plays an important role (e.g., Tyson and Preston-White 2000; Koseki et al. 2018; Koseki and Demissie 2018). Over the southeast coast, nearly half of annual rainfall is associated with ridging anticyclones (Engelbrecht et al. 2015; Engelbrecht and Landman 2016). The Mascarene anticyclone over the southwest Indian Ocean also plays an important role in moisture transport onto the interior plateau with the Drakensberg blocking deflecting northward the offshore flux of moisture coming from the Indian Ocean (Koseki and Demissie 2018). The Agulhas Current is potentially a source of moisture for the surrounding continent, and it creates a band of moisture above the current that forms a patch of cloud lines (Lee-Thorp et al. 1999; Rouault et al. 2000) south of Africa. The impact of the Agulhas Current on weather and climate was not well represented in earlier low-resolution 2.5° × 2.5° reanalyses (Rouault et al. 2003; Nkwinkwa Njouodo et al. 2018). Over the Agulhas Current the turbulent latent heat flux (also called the turbulent flux of moisture) from ocean to atmosphere increases considerably and is up to 5 times larger than over the surrounding ocean (Rouault et al. 2000, 2003). As winds blow from cool to warm sea surface temperature (SST) in this region, this enhances the turbulent heat fluxes, destabilizing the atmospheric boundary layer over the warmer SST and increasing vertical mixing, and therefore deepens the boundary layer above the Agulhas Current (Lee-Thorp et al. 1999; Rouault et al. 2000; Rouault and Lutjeharms 2000; Krug et al. 2018). Ultimately, this leads to a high flux of moisture toward the coast that penetrates inland when the wind blows from the Agulhas Current to the shore (Jury et al. 1997; Lee-Thorp et al. 1999; Rouault et al. 2000).

In a companion paper (Nkwinkwa Njouodo et al. 2018), we have used WRF atmospheric model simulations that realistically resolve rainfall over the Agulhas Current to show the importance of the underlying SST in anchoring rainfall above the current and in the adjacent coastal region. More specifically, we performed two simulations with the Weather Research and Forecasting (WRF) numerical model: the control run forced by 1/4° resolution Optimum Interpolation Sea Surface Temperature (OISST; Reynolds et al. 2007) and a second experiment forced by SST smoothed in order to remove the sharp SST gradient associated with the Agulhas Current and to decrease its temperature by about 1.5°C. Focusing on annual averaged rainfall, we showed that the core of the Agulhas Current is associated with a band of rainfall along the eastern coast of South Africa. The rainfall is collocated with the low-level wind convergence, SST Laplacian, and sea level pressure (SLP) Laplacian in a relation similar to that found over the Gulf Stream, and resembling the pressure adjustment mechanism (Minobe et al. 2008). Pioneering regional modeling studies by Reason and Mulenga (1999) using two years of a 2.5° × 2.5° low-resolution atmospheric general circulation model (AGCM), forced with a warm anomaly in the southwest Indian Ocean showed an increase in summer rainfall in South Africa. This was due to an increase in the flux of moisture from the southeast of South Africa and an increase in moisture convergence inland. Later, Reason (2001) used two experiments of 1-yr integration of the same AGCM, with SST input based on the 1° × 1° Reynolds SST. In one simulation, the author smoothed out the monthly climatological SST of the greater Agulhas region (an area that encompasses the Agulhas Current, the Agulhas Retroflection, and the Agulhas Return Current) to study the impact of the greater Agulhas Current system on winter and summer rainfall. Reason (2001) found that differences between the two experiments are more pronounced in winter than in summer. He showed the evidence for the importance of the greater Agulhas Current system for South Africa climate and weather. However, the low resolution of the model used did not capture the core of the Agulhas Current and therefore the high latent and sensible heat fluxes associated to the core. At least 1/3° resolution is needed to get the core of the current (Rouault et al. 2003; Rouault and Lutjeharms 2003) and the associated high sensible and latent heat fluxes.

Recent works have shown the ability of WRF to simulate southern African rainfall (Barimalala et al. 2018; Desbiolles et al. 2018, 2020). Barimalala et al. (2018) used 17 summers of integration to study the impact of Madagascar on southern African rainfall, with 10-km horizontal resolution. More relevant to our study, Desbiolles et al. (2018) used a 9-month integration of WRF in a wide domain (45°–5°S, 5°W–65°E). They showed that increasing the resolution of SST to an effective resolution of 20 km in the model to consider mesoscale ocean feature such as eddies led to regional change in rainfall, a decrease of the flux of moisture from tropical region to southern Africa, especially from the Mozambique Channel, and a change in the location of the ITCZ. Using the same model and configuration, Desbiolles et al. (2020) suggested that the Angola low is also intensified when considering the mesoscale ocean feature at the Angola Benguela Front, leading to important changes in regional rainfall, especially in Angola and Namibia. Jury et al. (1993) were the first to show that inland rainfall in South Africa is influenced by Agulhas Current temperature and its proximity to the coast. Later, Jury (2015) proposed that during El Niño–Southern Oscillation (ENSO) the Agulhas Current has a passive role in suppressing rainfall inland.

The aim of our paper is to extend our previous study to identify the seasonal impact of the Agulhas Current warm core on southern Africa. We make use of the two simulations from our previous study of Nkwinkwa Njouodo et al. (2018). The SST of the Agulhas Current is well represented in the control simulation whereas in the second the warm SST of the Agulhas Current is reduced by 1.2° to 1.5°C, through spatially filtering to reduce sharp SST gradients. In this paper we adopt the austral seasons, and from now on refer simply to summer (DJF), autumn (MAM), winter (JJA), and spring (SON). The rest of our study is structured as follows. Section 2 describes the data and experimental design used. Section 3 examines the surface parameters employed for this study. Section 4 investigates the mechanisms of the seasonal impact of the warm core of the Agulhas Current on precipitation. Section 5 discusses the results and concludes the study.

2. Data

We use the following observation-derived datasets: the high-resolution (0.1° × 0.1°) land based gridded climatology of Hewitson and Crane (2005) based on rain gauges from 1950 to 2000; the high-resolution (0.05° × 0.05°) Tropical Rainfall Measuring Mission Precipitation Radar (TRMM PR) climatology (Biasutti et al. 2012) based on the period 1998 to 2012; the 0.25° × 0.25° OISST (Reynolds et al. 2007) from 2001 to 2005; the Climate Forecast System Reanalysis (CFSR; Saha et al. 2010) from 2001 to 2005; and the latest European Centre for Medium-Range Weather Forecast (ECMWF) reanalysis (ERA5; Hersbach et al. 2020) from 1979 to 2020. Because the core of the Agulhas Current is about 80–100 km wide, 0.25° × 0.25° resolution is enough to represent the core of the Agulhas Current (Imbol Nkwinkwa et al. 2019). Using SST with a 1/3° resolution the core of the current is still present (Rouault and Lutjeharms 2003).

In addition, we use two experiments of the Weather Research and Forecasting (WRF) Model (Skamarock and Klemp 2008) to isolate the effect of the Agulhas Current warm core on the atmosphere (Nkwinkwa Njouodo et al. 2018; Koseki et al. 2018). The model domain extends from 17° to 43°S and from 8° to 52°E, with a 25 km × 25 km horizontal resolution. The delimitation of the study area is motivated by the investigation of the local impact of the Agulhas Current on South Africa rainfall. The model has 56 vertical eta-coordinate levels, with 22 levels below $\eta = 50$ (~100 hPa) to represent the lower atmosphere. The model outputs are 3-hourly. The two experiments cover the period from 2001 to 2005, with lateral boundary conditions from the ERA-Interim reanalysis (Dee et al. 2011). The experiments differ only in the surface boundary conditions: WRF-control (hereafter CTL) prescribes satellite-derived SST (Reynolds et al. 2007), while WRF-smoothed (hereafter SMTH) prescribes the same SST except spatially smoothed over the core of the Agulhas Current. The spatial filter used is based on a nine-neighbor grid method, applied 100 times (Koseki et al. 2018). The filter is given by NCAR Command Language (NCL) and is called smth9_Wrap (http://www.ncl.ucar.edu/Document/Functions/Contributed/smth9_Wrap.shtml). Compared to CTL, the SST in SMTH is 1.5°C colder over the Agulhas Current, leading to weaker turbulent latent and sensible heat fluxes. See Nkwinkwa Njouodo et al. (2018) for a detailed model description and validation.

3. Surface parameters

a. *Surface current, sea surface temperature, and latent heat flux*

The Agulhas Current speed has a relatively low amplitude in its annual cycle with a geostrophic current speed varying from 1.5 m s^{-1} in March to 1.3 m s^{-1} in July (Krug and Tournadre 2012). The recent study of Hutchinson et al. (2018) showed that the Agulhas Current is over 25% stronger in summer than in winter. The SSTs in the Agulhas Current system are several degrees Celsius warmer compared to the surrounding region (Fig. 1) and have a strong seasonality that is typical of the midlatitudes. The warmest temperature is about 25°C in summer around 32°S, with the highest SST occurring in February. The Agulhas Current causes a strong oceanic temperature gradient along the east coast of South Africa, creating low-level atmospheric instability and potentially enhancing atmospheric convection. In autumn, SST is quite similar to summer (Fig. 1b) because the SST is maximum in February and March. Austral winter is the season with the coolest SST in the Agulhas region (Fig. 1c). Spring SST is similar to winter SST, with the warmest SST along the coast, in the Agulhas Current (Fig. 1d). There is about 3°C difference in SST between the summer and winter along the Agulhas Current. The wind speed and the high SST gradient created by the core of the Agulhas Current causes a large amount of turbulent latent heat flux (LHF) and moisture transfer from ocean to atmosphere. Along the Agulhas Current, the LHF is maximum all year long (between 175 and 250 W m^{-2}), but with higher values in winter (Fig. 1g) and lower values in summer (Fig. 1e). In winter, relatively strong and cool westerly winds blow over the Agulhas Current. The cooler airmasses and stronger winds in winter than summer then explain the increased LHF in this season relative to summer. East of Port Elizabeth, the difference in specific humidity between the surface of the Agulhas Current, the function of SST, and the air masses advected above are more important in driving the variability of the LHF than the wind (Imbol Nkwinkwa et al. 2019). Moreover, in summer the wind is mostly easterly to northeasterly above the eastern part of the current. For a more detailed discussion on the annual cycle of the SST and the LHF in the Agulhas region, see Imbol Nkwinkwa et al. (2019). The authors compared some satellite-based LHF and reanalysis datasets. They found that the new higher-resolution climate reanalyses do capture the high LHF above the core of the Agulhas Current and that the WRF Model LHF compares well with those in Imbol Nkwinkwa et al. (2019).

Over the land, the maximum modeled LHF is in summer (~150 W m^{-2}) and the minimum in winter (~50 W m^{-2}), corresponding to an evaporation rate of ~5.3 mm day^{-1} in summer and ~1.8 mm day^{-1} in winter. Note that 1 mm day^{-1} of evaporation is equivalent to a loss of energy of 28 W m^{-2}.

b. *Precipitation*

We use the 50-yr climatology of South African precipitation from Hewitson and Crane (2005, hereafter HC05) to validate the simulated land rainfall of the WRF Model. HC05 use the conditional interpolation method. The first step of this method is to use the local precipitation distribution and to assign each day in the record to a particular synoptic state. The last step is to use each location where the rain is indicated and interpolate the precipitation amount (HC05). Although the model output is only 5 years, its climatology compares quite well with the 50-yr-long HC05 climatology.

South African precipitation ranges between 0 and 7 mm day^{-1}, with a maximum in summer in the southeast of the country (23°–25°S, 30°–31°E; Fig. 2a). Another maximum is around the Drakensberg region (29°–30°S, 29°–30°E). Meanwhile, the southwest of the country is arid in summer. During autumn, precipitation ranges between 0 and 3 mm day^{-1}, with a

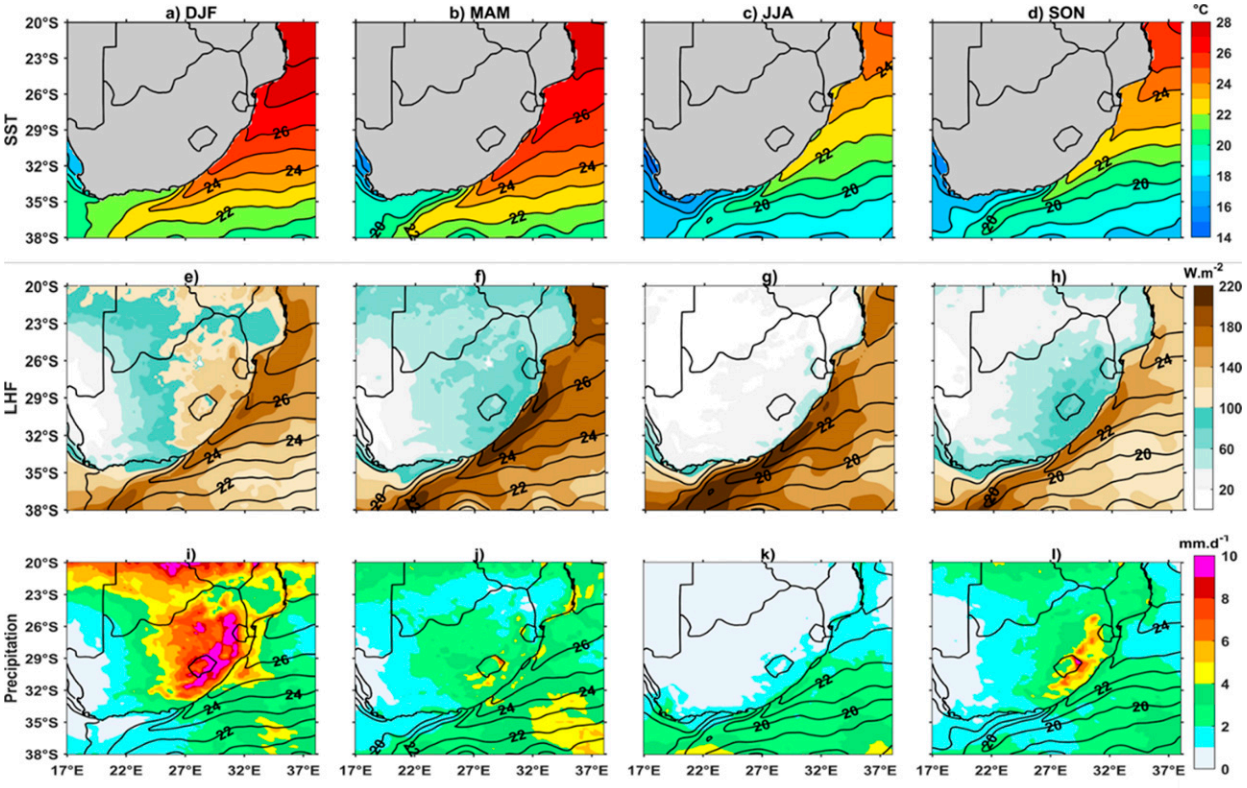

FIG. 1. Seasonal average of WRF-control experiment for (a)–(d) sea surface temperature (SST), (e)–(h) latent heat flux (LHF), and (i)–(l) precipitation for, from left to right, austral summer [December–February (DJF)], austral autumn [March–May (MAM)], austral winter [June–August (JJA)], and austral spring [September–November (SON)]. Black contours represent the SST with 1°C interval overlaid.

maximum along the south coast and the east coast of South Africa (Fig. 2b). This maximum lasts until winter, forming a rainband ranging from 1 to 2 mm day^{-1} (Fig. 2c). Winter is the rainy season over the Western Cape (31°–34°S, 18°–20°E), with precipitation up to 6 mm day^{-1}. Meanwhile, the rest of the country is arid. Spring is the transitional season between the winter and summer regimes and is marked by an increase in precipitation over the southeast of South Africa, with a clear maximum rainfall along the east coast, where the Agulhas Current is adjacent to the coast (Fig. 2d).

We use the 5 km × 5 km TRMM PR climatology to validate the WRF rainfall above the ocean and to compare with HC05 climatology for the rest of southern Africa (Fig. S1 in the online supplemental material). We note that the TRMM climatology is only available since 1998 while HC05 is 50 years and our model 5 years. TRMM also could suffer from the usual limitation in satellite remote sensing of rainfall. However, it is the highest resolution possible above the ocean. TRMM PR overestimates the summer terrestrial rainfall by 1 mm day^{-1} (Fig. S1a) compared to the climatology of HC05. However, TRMM PR underestimates precipitation along the inland coast by 2 mm day^{-1} compared to the former climatology, which shows a maximum rainfall along the coast. In TRMM PR, the highest summer precipitation is northeast of southern

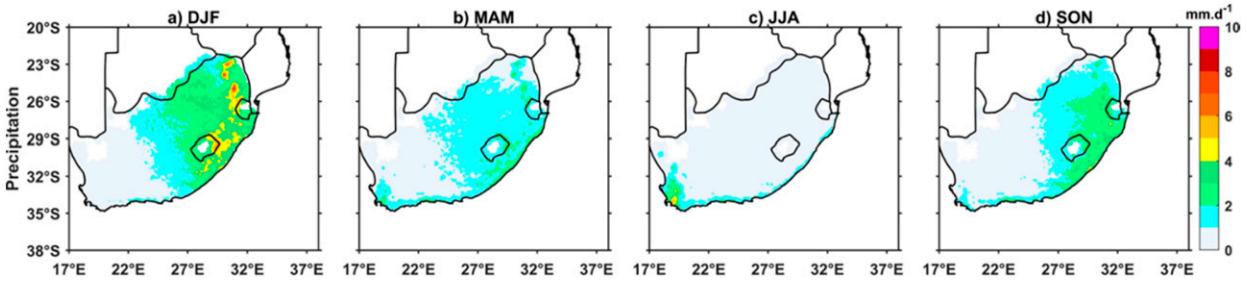

FIG. 2. Climatology of South Africa precipitation rate from 1950 to 2000 of the gridded averaged daily precipitation data from Hewitson and Crane (2005): from left to right, austral summer (DJF), austral autumn (MAM), austral winter (JJA), and austral spring (SON).

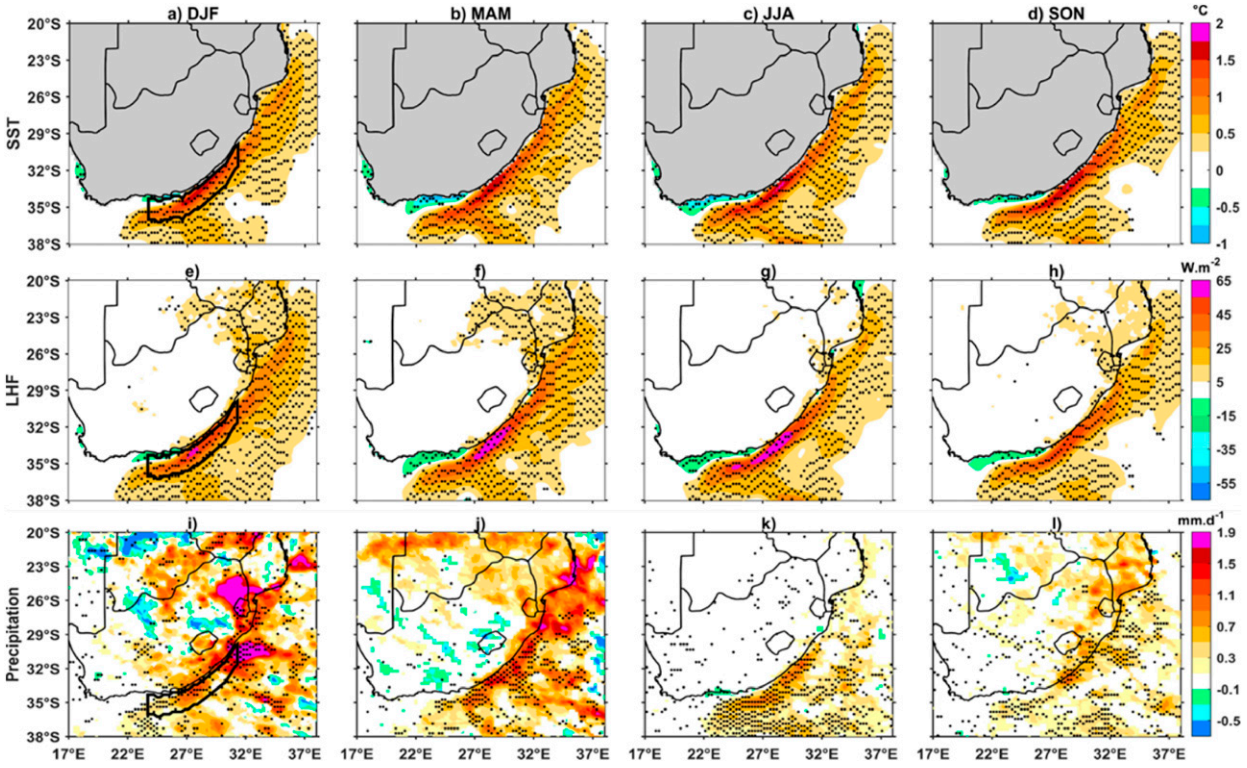

FIG. 3. As in Fig. 1, but for the mean seasonal differences between control and smooth experiments. Bold contours indicate the area between 23° and 31°E within a 2° coastal band. Shaded values significant at the 90% level are indicated by a black dot.

Africa. In autumn, terrestrial precipitation is also overestimated by 1 mm day^{-1} (Fig. S1b) compared to the climatology of HC05. Above the ocean, largest values of rainfall are found over the Agulhas region and the South Indian convergence zone (SICZ; e.g., Cook 2000). TRMM PR underestimates the winter rainfall over the Western Cape, and at the coast to the east (Fig. S1c). Over the ocean, the imprint of the Agulhas Current is clearly apparent in winter precipitation. In spring, precipitation is abundant over the landmass, east of South Africa (Fig. S1d). Analysis of TRMM PR frequency of rainfall (Figs. S1e–h) shows that the Agulhas Current is the region where it rains the most often considering all seasons.

CTL overestimates summer precipitation compared to the climatology of HC05 by 3 mm day^{-1}, east of South Africa (Fig. 1i). Along the coast, CTL captures the maximum rainfall seen in the former climatology. This might be due to the strong sensitivity of simulated precipitation to the terrain (e.g., Pohl et al. 2014; Koseki et al. 2018) or the difference in climatology. Summer precipitation is well simulated above the Agulhas Current by CTL when compared with TRMM-PR (Figs. S1a,e). During autumn, CTL precipitation can reach 6 mm day^{-1} (Fig. 1j). As in summer, the model overestimates land precipitation by 3 mm day^{-1} in autumn, and the rainfall pattern is similar to summer, but with a lower amplitude. However, the model underestimates maritime precipitation in autumn. In winter above the Agulhas, precipitation ranges between 3 and 4 mm day^{-1}. Thus, CTL underestimates the maritime precipitation by 2 mm day^{-1} above the Agulhas Current (Fig. 1k) compared to TRMM PR (Fig. S1c). In spring, CTL overestimates the terrestrial and maritime precipitation (Fig. 1l) compared to the climatology of HC05 and TRMM PR respectively.

To summarize, the WRF Model overestimates the land precipitation compared to HC05 for all seasons, and underestimates the maritime precipitation in autumn, winter, and spring, compared to the rain frequency of TRMM PR (Figs. S1e–h). However, the main features and seasonality of southern Africa and adjacent rainfall are relatively well simulated. Thus, the WRF Model compares reasonably well with observations and can be used for our seasonal analysis.

To assess the impact of short runs we present the mean seasonal SST, LHF, and precipitation of ERA5 (Fig. S2). Averages are done on a 42-yr period, from 1979 to 2020. We notice that the seasonality of each parameter is quite similar to the CFSR reanalysis (Nkwinkwa Njouodo 2018, chapter 5) and to our modeling results but with a lesser amplitude.

4. Influence of the Agulhas Current on precipitation

a. SST, LHF, and precipitation differences between WRF experiments

In this section, we look at the seasonal influence of the warm SST of the Agulhas Current on southern Africa rainfall based on the difference between CTL experiment and the experiment with a smoothed SST (SMTH). The SST difference between the two simulations is up to 1.5°C along the coast and

presents a weak seasonality (Figs. 3a–d). The maximum difference is found in the core of the Agulhas Current, around 33°–35°S and 27°–30°E (Eastern Cape). Smoothing the SST reduces the Agulhas Current SST in summer by 1°C in the northeast, and 1.5°C along the coast. Smoothing the SST also leads to a 1°C cooler SST along the coast of the Western Cape region (31°–33°S, 18°E) and the South Coast (34°S, 20°–26°E) for each season. However, the absolute value of the SST and of the LHF in upwelling region are quite low so the impact on weather of the coastal smoothing is not important for our study. Indeed, the difference in LHF along the West and South Coast between control and smooth is 5 times lower in absolute value than above the Agulhas Current (Figs. 3e,f).

The LHF differences between the two simulations exhibit a maximum in the Agulhas Current in all seasons (Figs. 3e–g), consistent with the seasonal SST differences (Figs. 3a–d). These differences can reach 65 W m^{-2}. Thus, reducing the SST by ~1.5°C leads to a 65 W m^{-2} loss of LHF (equivalent to an evaporation rate of 2 mm day^{-1}). Over the land, north of South Africa, the LHF difference is about 15 to 25 W m^{-2} in summer, autumn, and spring (Figs. 3e,f,h). Along the West and South Coast where the SST is increased by the smoothing the maximum difference is 10 W m^{-2}.

The Agulhas Current influences precipitation patterns in all seasons, as illustrated by the differences in simulated precipitation rate in the two WRF experiments (Figs. 3i–l). The rainband anchored by the Agulhas Current is mostly due to cumulus convective rain (not shown). Maximum differences in terrestrial precipitation are found in summer over the northeast of South Africa, around Mpumalanga (24°–27°S, 30°–33°E), but the statistical significance is weak (Fig. 3i). Maximum differences in oceanic precipitation occur also in summer off Durban (30°–32°S, 31°–33°E) and above the Agulhas Current. In autumn, positive precipitation differences along the coast extend far west inland between 20° and 23°S (Fig. 3j). Again, the statistical significance is weak. In winter, the land precipitation is almost identical in both simulations and close to zero. Positive precipitation differences occur along the east coast (Fig. 3k) and above the core of the Agulhas Current, coinciding with the locations where the SST and LHF differences are maximum. In many respects, our study shows results similar to those of Reason (2001). The author investigates the potential influence of the greater Agulhas Current system on regional atmospheric circulation. He showed that smoothing out the SST of the greater Agulhas Current system results in a stronger LHF differences in winter than summer, with higher associated precipitation differences above the SST anomalies in winter; there were also differences in precipitation above land for both seasons.

In spring, maximum precipitation differences are found along the coast and northeast of southern Africa (Fig. 3l). Compared to CTL, the change in precipitation over the Agulhas Current can be as high as 35% during the wettest seasons (summer and autumn) and as high as 25% during the driest seasons (Fig. S3). Thus, the influence of the Agulhas Current on precipitation follows the seasonal cycle, being greatest during the wettest seasons and least during the driest seasons. These results indicate that reducing the temperature of the Agulhas Current has the overall effect of decreasing the precipitation above the Agulhas Current in all seasons where the current is adjacent to the coast, and over parts of southern Africa in summer, autumn, and spring. Koseki et al. (2018) showed that with smoothened warm SST caused by the Agulhas Current, the coastal rainfall is diminished to some extent due to less evaporation along the Agulhas Current. However, it is not clear if the LHF is the main factor controlling rainfall seasonality above the current. Comparing for example autumn and winter, both have similarly strong LHF, but there is much more rainfall in autumn (Fig. 3). In summer, there is more rainfall, but LHF is even less. However, the SST is higher and the precipitable water content could therefore be higher leading to more rainfall above the current. The changes in precipitation between the experiments were to the first order shown to be linked to the pressure adjustment mechanism at annual scale by Nkwinkwa Njouodo et al. (2018). Does this mechanism occur similarly in the different seasons? What controls the seasonal differences in the impact over the continent? Further analyses to answer these questions are done in the following section.

b. *Analysis of the pressure adjustment mechanism*

We examine the relationship between the sign-reversed SST Laplacian, the 10-m wind convergence, and the SLP Laplacian for the difference between both simulations for each season. The SST Laplacian, wind convergence, and SLP Laplacian are linked by the pressure adjustment mechanism (Lindzen and Nigam 1987; Minobe et al. 2008; Nkwinkwa Njouodo et al. 2018; Crespo et al. 2018), following the equations of the pressure adjustment, in which the SST modifies the marine atmospheric boundary layer, and the resultant pressure gradients produces wind convergence over warm SSTs and wind divergence over cold SSTs. The momentum equation can be approximated for a frictional boundary layer as follows:

$$\begin{cases} \varepsilon u - f v = -\dfrac{p_x}{\rho_0} \\ \varepsilon v + f u = -\dfrac{p_y}{\rho_0} \end{cases}, \tag{1}$$

where x and y are the zonal and meridional coordinates; u and v are the zonal and meridional surface wind; and ρ_0, p, ε, and f are the density, the pressure, the constant damping coefficient, and the Coriolis parameter, respectively. The relationship between the surface wind convergence and the SLP Laplacian is linear:

$$-\rho_0(u_x + v_y) = (p_{xx} + p_{yy})\frac{\varepsilon}{(\varepsilon^2 + f^2)}. \tag{2}$$

Equation (2) can be derived from Eq. (1). The model assumes that SST and the temperature of the atmospheric boundary layer to be closely related to each other on monthly and longer time scales, adjusted through turbulent fluxes and atmospheric mixing (Lindzen and Nigam 1987). Moreover, satellite observations have such an influence on the Agulhas Current (Krug et al. 2018).

The Laplacian acts as a high-pass spatial filter and highlight the regions with strong gradients such as the Agulhas Current.

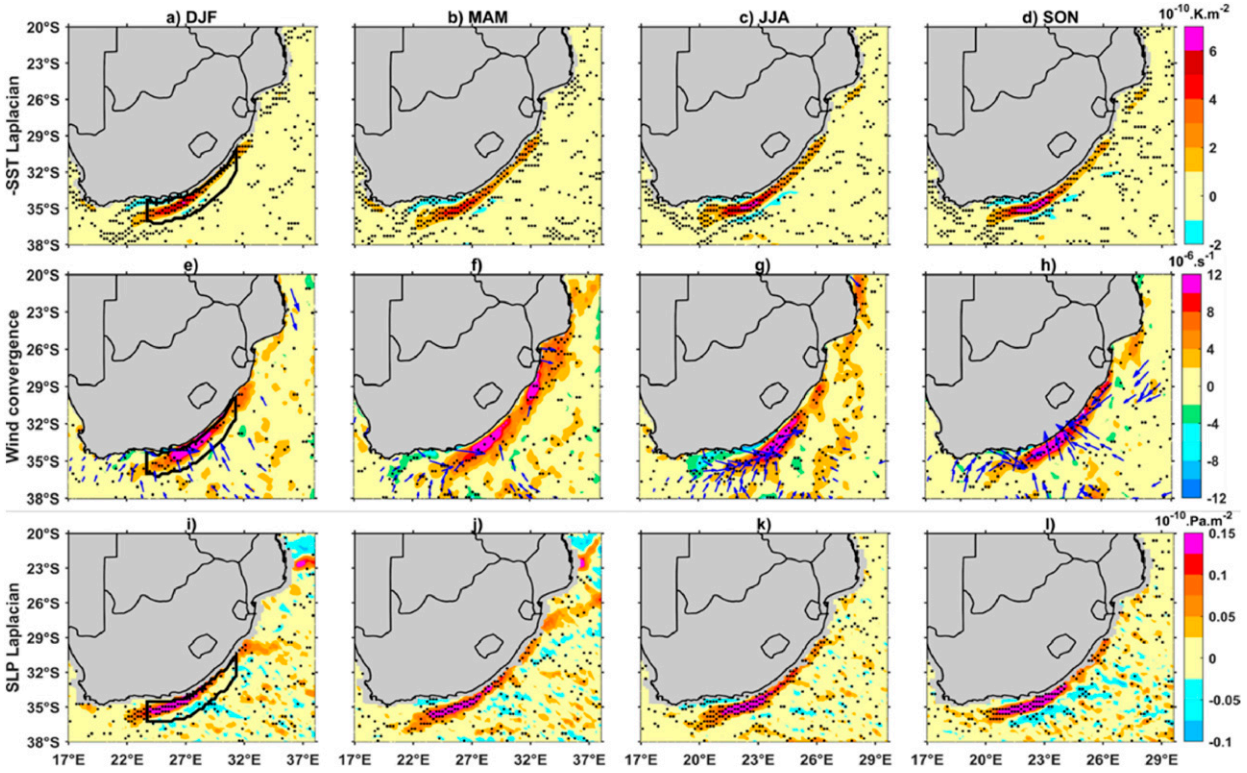

FIG. 4. As in Fig. 1, but for the mean seasonal differences between control and smooth experiments: (a)–(d) sign-reversed sea surface temperature Laplacian and (e)–(h) wind convergence (positive values). Superimposed blue arrows are the 10-m wind direction difference between the two simulations. (i)–(l) Sea level pressure Laplacian. Bold contours indicate the area between 23° and 31°E within a 2° coastal band. Shaded values significant at the 90% level are indicated by a black dot.

The differences in the sign-reversed SST Laplacian along the eastern coast of South Africa show a strong gradient for each season (Figs. 4a,b). The result is similar to the one described at annual scale by Nkwinkwa Njouodo et al. (2018). The SST Laplacian differences are large along the coast for each season (between 22° and 32°E). The highest values of about 6×10^{-10} K m^{-2} are found in winter and spring.

Figures 4e–h illustrate the difference in wind convergence (shading) and in the wind at 10 m (vectors) between control and smoothed experiments. In all seasons the wind convergence differences are stronger above the Agulhas Current compared to the surrounding water. The maximum values range between 8×10^{-6} and 12×10^{-6} s^{-1}. The wind direction changes show that in autumn and winter the increased convergence in CTL is mainly from the alongshore component, while in summer and spring there is also a substantial cross-shore component.

The differences in the SLP Laplacian (Figs. 4i,j) show some similarities to the SST Laplacian and wind convergence difference patterns in all seasons. These results indicate that pressure adjustment to SST gradients around the Agulhas is important for surface wind convergence in all seasons. The SLP Laplacian differences are collocated with the precipitation differences over the Agulhas Current. The patterns of the sign reversed SST Laplacian, wind convergence, and SLP Laplacian differences show similarities with those of the annual mean analysis. Therefore, this indicates that the pressure adjustment acts in every season and contributes to enhancing seasonal precipitation above the current. There are also larger LHF differences in this location that can directly affect the stability, specific humidity, and precipitable water in the lower troposphere (Fig. 3); this could also induce a surface wind divergence and convergence (Takatama et al. 2012). Therefore, seasonally reducing the Agulhas Current SST leads to a reduction of the dynamical and thermodynamic factors for enhancing precipitation over the Agulhas Current. Supporting these modeling results, the CFSR reanalysis shows patterns in LHF, SLP Laplacian, and wind convergence similar to those of the WRF numerical experiments (Nkwinkwa Njouodo 2018, chapter 5). Moreover, Fig. S4 represents the seasonal averages of ERA5 SST Laplacian, wind convergence, and SLP Laplacian for a longer period from 1979 to 2020. Results are similar to CFSR reanalysis, and the WRF control experiment. This comparison indicates that five years of data can resolve the key seasonal differences.

To quantify to what extent the seasonal precipitation differences can be explained by these factors, we evaluate the seasonal mean differences between CTL and SMTH runs of precipitation, SST, LHF, SST Laplacian, wind convergence, and SLP Laplacian differences. The parameters are averaged between 23° and 31°E and within the 2° width coastal band. The selected area is illustrated by the bold line

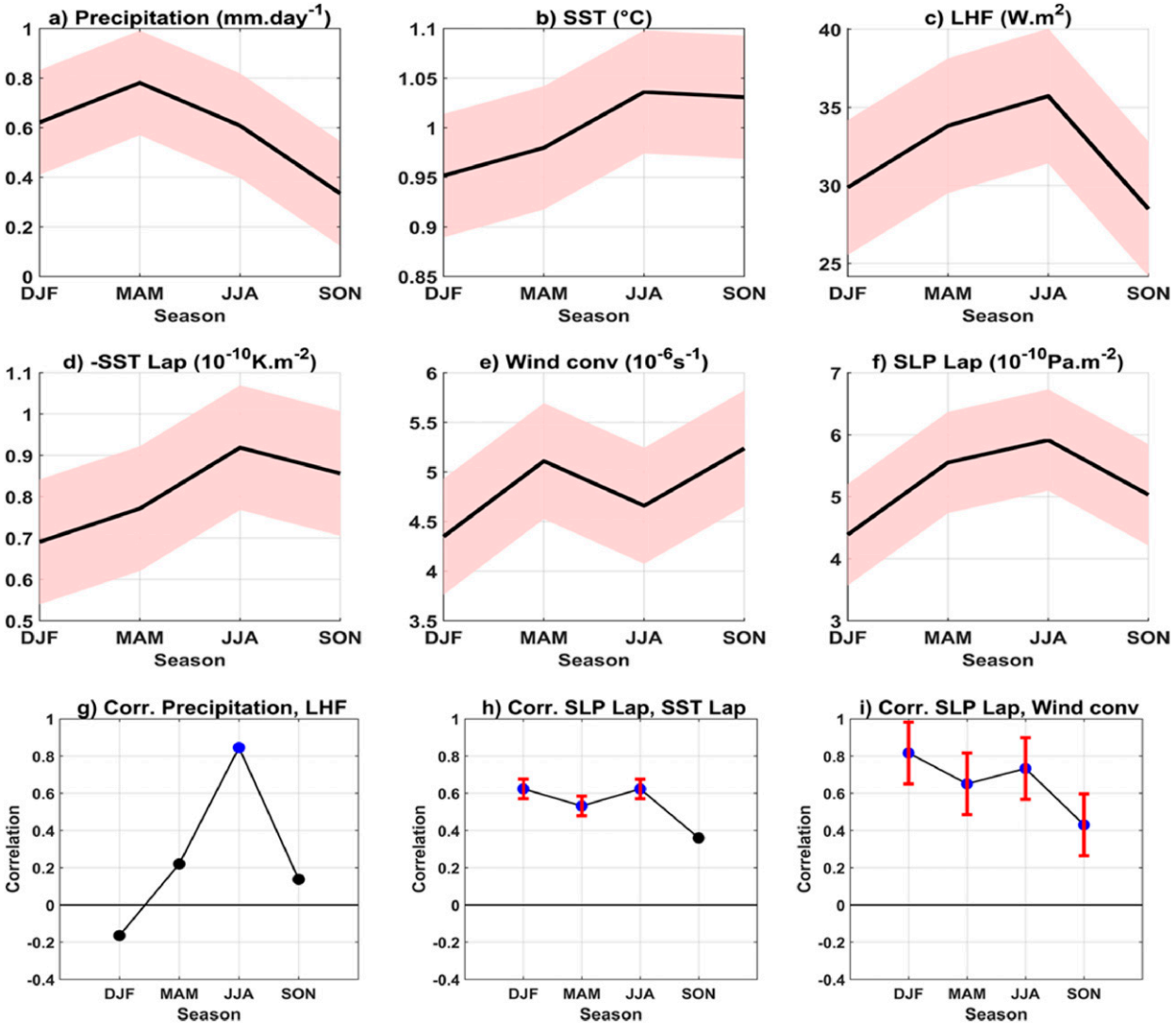

FIG. 5. Seasonal mean differences between WRF-control and smooth SST experiments averaged between 23° and 31°E and within the 2° width coastal band for (a) precipitation, (b) SST, (c) latent heat flux, (d) sign-reversed SST Laplacian, (e) wind convergence, and (f) sea level pressure (SLP) Laplacian. Shaded areas represent ±1 standard deviation. Monthly correlation analysis between (g) precipitation and latent heat flux, (h) SLP Laplacian and SST Laplacian, and (i) SLP Laplacian and wind convergence. Blue (black) dots represent significant (not significant) correlations (see Table 1 for values). The significance is at the 90% level. Error bars in red are ±1 standard deviation.

outlined patch in Figs. 3 and 4, where the Agulhas Current has the highest speed.

In summer, the wind convergence differences are weaker (Fig. 5e), and the differences in SLP Laplacian are lowest (Fig. 5f). Correlations between the SLP Laplacian and wind convergence are greater than in autumn. Pointwise correlation between precipitation and LHF is 20.16 and not statistically significant (Fig. 5g and Table 1). Thus, the change in summer precipitation above the Agulhas Current could be due mainly to the pressure adjustment mechanism compared to the thermodynamic effect measured by the LHF. We reach the same conclusion for spring precipitation.

During autumn, wind convergence differences are stronger (Fig. 5e) and the SLP Laplacian differences higher compared to summer. Correlation between SLP Laplacian and wind convergence is lower (0.65 ± 0.12) and significant at the 90% level (Fig. 5i and Table 1). In contrast, the correlation between precipitation and LHF is lower (0.22). Thus, changes in autumn precipitation appear more related to changes in the pressure adjustment mechanism.

In winter, precipitation differences range between 0.4 and 0.8 mm day^{-1}. The LHF contribution to precipitation is found to contain a wintertime maximum, and the dynamical effect to explain precipitation differences is high (relation between SLP Laplacian and wind convergence). We suggest that the precipitation changes in winter are due to the thermodynamic effect with a correlation of 0.85 between precipitation and

TABLE 1. Statistical value of monthly correlation from Fig. 5. The significance is at the 90% level. The domain covers 23° and 31°E and within the 2°-width coastal band. STD = Standard deviation.

Season	Correlation: precipitation vs latent heat flux	Correlation: SLP Laplacian vs SST Laplacian with STD	Correlation: SLP Laplacian vs wind convergence with STD
Summer (DJF)	−0.16	0.62 ± 0.05	0.82 ± 0.17
Autumn (MAM)	0.22	0.53 ± 0.05	0.65 ± 0.17
Winter (JJA)	0.85	0.62 ± 0.05	0.73 ± 0.17
Spring (SON)	0.14	0.36 ± 0.05	0.43 ± 0.17

LHF, and the pressure mechanism with a correlation of 0.73 ± 0.17 between SLP Laplacian and wind convergence (Table 1).

The seasonal variations in rainfall differences broadly follow the seasonal difference in rainfall, with most rainfall occurring in summer and autumn, and least in winter and spring. Although the relative importance of dynamical and thermodynamical influences vary with season, they do not correspond closely to the seasonal differences in rainfall. Thus, the seasonal differences may be more related to the large-scale factors that determine seasonality, such as the atmospheric circulation discussed in the next section and the temperature of the Agulhas Current, which is warmest in summer and autumn, and coldest in winter and spring. This will have an impact on the specific humidity and the precipitable water in the lower troposphere above the current, thereby modulating the local dynamical and thermodynamical influences on rainfall. One reason for differences in low-level convergence and rainfall response to the underlying SST in autumn and winter may be related to synoptic-scale weather (Parfitt and Czaja 2016; Parfitt et al. 2016; O'Neill et al. 2017); this could weaken the relation between SLP Laplacian and wind convergence.

In summer, the coastal rainfall is not caused only by the SST-induced wind convergence over the Agulhas Current, being confined to the ocean. Koseki et al. (2018) indicated that the impact of the SST front on the coastal region could be the result of the diurnal cycle. The authors suggested that variations in rainfall are associated with the daily residual local circulations: when the terrestrial precipitation is dominant, the onshore and uphill breeze systems are formed around the Drakensberg, midrange mountain, and coastal orography of South Africa.

c. *Atmospheric parameters*

1) GEOPOTENTIAL HEIGHT

We now focus on austral summer because the southeast portion of southern Africa gets most of its precipitation in summertime and the modeled impact of the Agulhas Current over the continent is the largest. Figures 6a and 6c represent the geopotential heights at 950 and 700 hPa in summer, simulated in the control experiment. The south Indian Ocean high pressure system is apparent in the Indian Ocean at 950 hPa. At 700 hPa, geopotential heights are lower south of 30°S corresponding to the midlatitude westerly systems, while the Botswana high pressure system (Driver and Reason 2017) can be seen to the north. In austral winter, the land is cold and the geopotential height is higher over the continent (Nkwinkwa Njouodo 2018, chapter 5), and this strengthens the subsidence that is not favorable for precipitation.

The analysis of the vertical velocity averaged between 950 and 800 hPa shows a rising motion for each season, with almost the same intensity (Fig. S6 of Nkwinkwa Njouodo et al. 2018). The observed vertical motion is collocated with the increased rainband along the coast. In summertime, the Agulhas Current warm core drives a significant weakening of the high pressure systems.

Figures 6b and 6d show the geopotential height differences between CTL and SMTH. At 950 hPa negative geopotential height differences are present above the Agulhas Current and surrounding ocean triggered by the SST differences (Fig. 6b), while at 700 hPa the negative differences are mostly above the continent (Fig. 6b). These differences indicate that without the warm SST of the Agulhas Current part of the Indian Ocean high pressure system and continental high pressure would be stronger, and thereby would reduce continental rainfall. The previous result is also observed in autumn and to a lesser extent in spring (not shown).

Nkwinkwa Njouodo et al. (2018) have shown that the rainfall response to the warm core of the Agulhas Current is associated with an overlying vertical circulation confined to the region below 650 hPa. Quasigeostrophic theory indicates that in the midlatitudes, diabatic heating at these levels is balanced by advection of cold air from higher latitudes, which implies the development of a low pressure anomaly and cyclonic circulation anomaly to the east of the diabatic heating (Hoskins and Karoly 1981; Kushnir et al. 2002; Sutton and Mathieu 2002). Consistent with this, there is a low pressure anomaly at lower levels to the east of the rainfall maxima over the Agulhas warm core (Figs. 3j and 6b). As explained below this induces a positive precipitation anomaly over the landmass, and along the east coast of South Africa (Fig. 3i).

The diabatic heat anomalies associated with this rainfall can further alter the geopotential height and circulation response. In particular, they appear to drive the low pressure anomalies around 25°S at lower levels. The low pressure anomaly at 700 hPa around 25°S is located just above the Drakensberg escarpment. The westerly winds at the mentioned latitude are blocked at lower levels by orographic barrier (Koseki and Demissie 2018) and may support upward propagating Rossby waves. The SLP anomaly pattern is around 20° in longitude (Figs. 6b,d), corresponding to a wavelength of 40° or wavenumber 9. At 25°S (30°S), Rossby waves of this scale would travel westward with a phase speed of 9 m s^{-1} (7 m s^{-1}). Given the simulated zonal winds (not shown), Rossby waves could

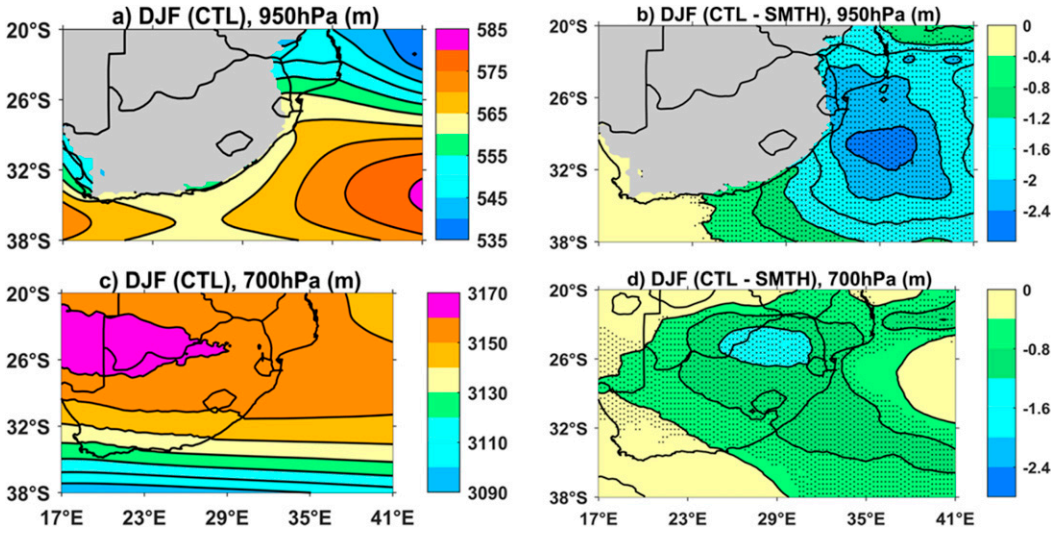

FIG. 6. Summer (DJF) geopotential heights simulated by WRF-control (CTL) experiment at (a) 950 and (c) 700 hPa, with (b),(d) the corresponding geopotential height differences between WRF-control and WRF-smooth. Black dots in (b) and (d) represent the significance at the 90% level.

propagate to around 700 hPa at 25°S, but they would be trapped to below 950 hPa at 30°S. According to these theoretical considerations, the westward tilting structure of geopotential height from 950 to 700 hPa may be partly caused by forced midlatitude Rossby wave (e.g., Holton and Hakim 2012).

A similar geopotential height structure is found in autumn, and to a lesser extent in spring. Thus, for summer, autumn, and spring our modeling results indicate that the warm SSTs of the core of the Agulhas Current off the southeast coast act to decrease pressure over South Africa.

As discussed in the previous section, it is difficult to relate the local dynamic and thermodynamic effects to the seasonal differences in rainfall. Rather, the reduced rainfall response in spring is probably due to the lower SST of the Agulhas Current (Figs. 1c and 5). Moreover, the South Indian anticyclone is higher and therefore weakens the rainfall. Another possibility is a change in the track, frequency, and intensity of transient weather systems such as fronts, which contribute to the tropical temperate troughs that bring most of the summer rainfall (see Reason 2001). Over the land, the low pressure anomaly difference does not appear in winter (not shown). Over the ocean the atmospheric large-scale response to the Agulhas Current warm core is limited to 850 hPa (not shown).

2) MOISTURE FLUX

To further understand the impact of the Agulhas Current on summertime continental precipitation, we compute the horizontal moisture flux intensity. This is defined as a product of the specific humidity and the wind, following the equation

$$\text{Moist}(uq, vq) = \sqrt{(uq)^2 + (vq)^2}, \tag{3}$$

where "Moist" is the moisture flux intensity, q is the specific humidity, and u and v are the zonal and meridional wind components, respectively. Moisture flux intensity is then computed at 950 and 700 hPa for the summer season (Fig. 7). At 950 hPa, the gray part above the continent is due to the presence of the continental plateau and escarpments at the coast (Fig. 7a).

At 950 hPa, an intense moisture flux originating from the Indian Ocean penetrates southern Africa (Fig. 7a). Part of this moisture flux flows along the coast just above the Agulhas Current before deflecting poleward. This westward moisture flux is associated with the Indian Ocean high pressure system, blocked by the Drakensberg (Koseki et al. 2018). The western Indian Ocean is the major moisture source for southern Africa (Vigaud et al. 2007). At 700 hPa, the moisture flux follows the westerlies and originates from the Atlantic Ocean then leaves the landmass toward the coast (Fig. 7c). The South Atlantic is considered as a secondary source of moisture for southern African climate (D'Abreton and Lindesay 1993; Cook et al. 2004; Reason et al. 2006; Vigaud et al. 2009). A bit of moisture leaving the continent, penetrates the continent from the east in an anticyclonic circulation. In autumn, winter and spring, the horizontal distribution of the moisture flux is quite similar to summer season, but with a reduced intensity. The moisture flux transport has the same direction as in summer. The moisture flux differences between control and smooth SST run, although only statistically significant at the 90% level (Figs. 7b,d) are consistent with the precipitation differences in summer (Fig. 3a). The moisture flux differences follow the geopotential height differences (Fig. 6). A 1.5°C warm SST creates up to $8\,\text{g}\,\text{kg}^{-1}\,\text{m}\,\text{s}^{-1}$ more moisture flux from the south in CTL than in SMTH, southwest of the Indian Ocean and along the east coast (Fig. 7a). The Agulhas Current therefore favors a cyclonic moisture flux anomaly leading to larger import of moisture from the south and in particular the band of moisture created by the Agulhas Current and larger export of moisture from the northeast of the continent at 950 hPa.

At 700 hPa (Fig. 7d), the differences in moisture flux follow the differences in the geopotential height field (Fig. 6d). We

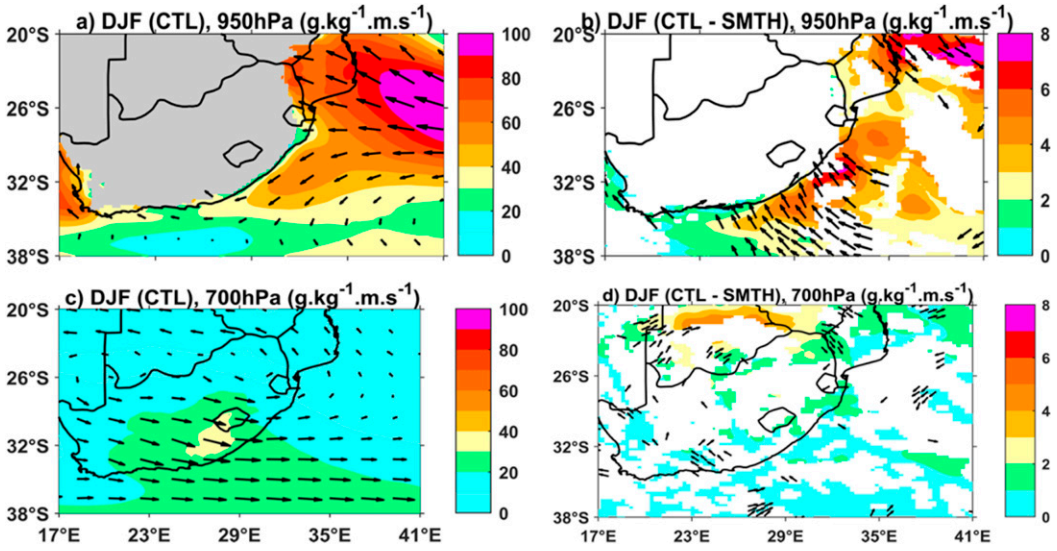

FIG. 7. As in Fig. 6, but for the moisture flux simulated by WRF-control (CTL) experiment at (a) 950 and (c) 750 hPa, with (b),(d) the corresponding moisture differences. Arrows represent the direction of the moisture transport every 1.5°. Colors in (b) and (d) represent the significant area at the 90% level, and the arrows are the moisture vector differences.

propose that it is the increase in moisture flux from the Agulhas Current that leads to more rainfall inland: this will lower the geopotential height and further create cyclonic motion, which will add further moisture inland. In other words, a 1°–1.5°C decrease in the Agulhas Current system SST decreases the inflow of moisture flux from the south and the southeast that more than compensates for the loss of moisture to the northeast. The absence of marked difference of moisture flux at 500 hPa (not shown) indicates that the convection is shallow within the air column. However, we observe a cyclonic moisture flux transport over the land area. The difference results (Figs. 7b,d) might not be the same if we had chosen a larger domain that could directly represent all the moisture sources mentioned above.

In autumn and spring, the mean circulation shows key differences compared to summer (not shown). The onshore wind is much reduced, and so the moisture transport to South Africa is less. In a similar way, the response over land is much weaker, even if we have a similar mechanism to summer. On the contrary, there is no signal of the moisture flux difference in wintertime. Thus, reducing the SST of the Agulhas Current does not have an impact on the precipitation over South Africa in austral winter.

5. Discussion and summary

In this study, we have investigated the seasonal impact of the Agulhas Current using satellite rainfall estimate and two experiments of the WRF regional model. We have first validated the WRF precipitation using a 50-yr climatology of Hewitson and Crane (2005) for land precipitation, and using TRMM PR for maritime rainfall. WRF underestimates the maritime precipitation mainly above the Agulhas Current. This could be because the SST gradients associated with the current are underestimated in WRF simulation. WRF overestimates the land precipitation for all seasons, which might be due to the sensitivity of WRF to the topography, a common issue in regional climate modeling (e.g., Nikulin et al. 2012; Pohl et al. 2014; Koseki et al. 2018). In general, annual mean rainfall is overestimated by regional climate models over South Africa (Favre et al. 2016) and also by global ocean–atmosphere coupled models (Dieppois et al. 2016). Despite these deficiencies, regional climate models have been demonstrated to simulate the main features of the annual cycle in circulation patterns and rainfall realistically, across the southern African region (Engelbrecht et al. 2015).

Our experiments revealed that the Agulhas Current has a pronounced seasonal influence on precipitation that acts to amplify the seasonal cycle. Over land there is a more widespread impact of the Agulhas Current in summer and autumn, which are the wettest seasons. A more realistic Agulhas Current as in CTL leads up to 45% (Fig. S3) increase in precipitation in summer and autumn compared to SMTH experiment. During winter, the land is arid and there is little influence of the Agulhas Current SST on southern African rainfall. In spring, precipitation differences are less compared to summer and autumn. Along the east coast of South Africa and over the adjacent Agulhas Current, the highest differences in precipitation occur in summer and autumn (Figs. 3a,b and 5a). During spring, the Agulhas Current SST has a modest influence on coastal precipitation. In wintertime, positive precipitation differences are pronounced only over the Agulhas Current (Fig. 3c), where the SST and LHF differences are maximum as also shown by Reason (2001) for the greater Agulhas Current system.

We have investigated the mechanisms for seasonal influence of the Agulhas Current on low-level wind convergence and maritime precipitation. We found that the SST Laplacian, SLP

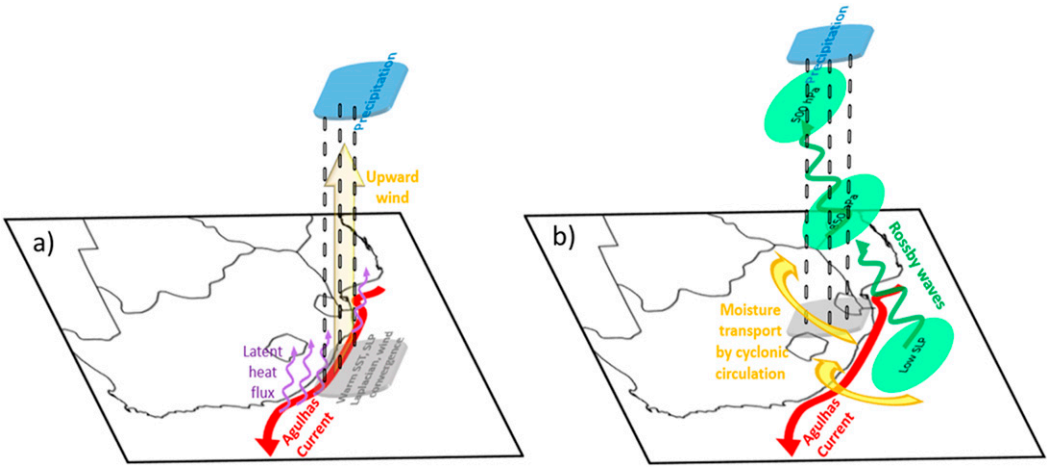

FIG. 8. Mechanisms of precipitation occurrence. (a) Along the coast and above the Agulhas Current (red), maritime precipitation is partly due to the release of latent heat flux (purple) by the current, and the relation between SST Laplacian, SLP Laplacian, and low-level wind convergence (gray) that will enhance precipitation. The upward wind velocity (yellow arrow) is shallow (below 500 hPa) and is associated with the wind divergence. Thus, a precipitation band (blue) forms over the Agulhas Current in all seasons. (b) Inland precipitation is caused by increased moisture flux (yellow arrows) from the Agulhas Current to the land, associated with a cyclonic motion. The northwestward tilted structure given by the geopotential height may be associated with vertically propagating Rossby waves around 25°S (green) from 950 to 700 hPa. The shadow inland represents the affected wet region. This mechanism acts most strongly in summer but is also present in autumn and spring.

Laplacian, and wind convergence in all seasons are consistent with the annual mean analysis (Nkwinkwa Njouodo et al. 2018). The link among these variables is enhanced in summer. Therefore, this indicates that the pressure adjustment to SST gradients is important for surface wind convergence; it suggests a dynamical mechanism for the collocation of precipitation over the Agulhas Current along the coast of South Africa during this season. In summertime, the coastal rainfall is also explained by the diurnal cycle as shown by Koseki et al. (2018). In autumn and winter there is a good relation between SLP Laplacian and wind convergence, thereby indicating that the pressure adjustment is important. In winter, a significant relation is found between LHF and precipitation that is weakly present in summer, autumn, and spring (Table 1). Furthermore, the LHF released above the Agulhas Current presents a summer and spring minimum, but an autumn and winter maximum (Fig. 5). These suggest that thermodynamic ocean–atmosphere interactions are important for precipitation over the Agulhas Current in winter. In summer and autumn, the Agulhas Current modifies the general circulation, which leads to an influx of moisture inland, increasing the rainfall. These two mechanisms act together to enhance the seasonal cycle of precipitation over southeastern Africa and the adjacent Agulhas Current (Fig. 8a). Figure 8 represents the mechanisms of precipitation occurrence along the coast (above the Agulhas Current) and inland precipitation. The northwestward tilted structure given by the geopotential height may be associated with vertically propagating Rossby waves around 25°S (Fig. 8b) from 950 to 700 hPa, and this gives the structure resembling a northwest trough undercut by a ridging anticyclone. The shallow diabatic heating from precipitation over the Agulhas Current induces a low pressure anomaly to its east, and thereby induces anomalous moisture transport and rainfall farther north and over the coastal regions of southern Africa. These may force vertical propagating Rossby waves at 25°S. This mechanism acts most strongly in summer but is also present in autumn and spring.

Our work gives support to the study of Jury et al. (1993), which estimated that the rainfall along the eastern coast of South Africa is positively correlated with the temperature of the Agulhas Current. However, it does not support his second hypothesis stating that rainfall was anticorrelated with the distance from the current to the coast. This could be due to the resolution of our experiment or simply because there is a west to east gradient in rainfall in South Africa unrelated to the vicinity of the current. While our study discusses the climatological feature of the Agulhas SST and precipitation over eastern South Africa, Jury (2015) has suggested that the variability of the Agulhas SST and precipitation over eastern South Africa are connected to the positive phase of ENSO and that the Agulhas Current has a passive role in suppressing rainfall in South Africa. Our relatively short experiment does not allow us to single out enough El Niño years. It would be interesting to explore how the impacts of Agulhas SST can be modulated during ENSO events compared to the climatology during summer in a longer integration.

The reason for the seasonal variations in the dynamic and thermodynamic influences of the Agulhas Current is still an open question. Considering another region, the study of Minobe et al. (2010) shows that variations in the importance of the pressure adjustment mechanisms occur over the Gulf Stream proper region: low-level wind convergence is weak and

TABLE 2. Summary of mechanisms activated for each season: italic and bold for strong, plain text (not italic/bold) for weak, and 0 for no mechanism. PAM = pressure adjustment mechanism.

Season	Precipitation above the Agulhas Current and coastal area	Precipitation inland
Summer (DJF)	***PAM*** + LHF	***Shallow heating*** + ***Rossby wave***
Autumn (MAM)	***PAM*** + LHF	***Shallow heating*** + ***Rossby wave***
Winter (JJA)	***PAM*** + ***LHF***	0
Spring (SON)	PAM + LHF	Shallow heating + Rossby wave

convection is deep in summer, whereas in winter low-level wind convergence is stronger and convection is shallow. These differences are due to different types of dynamics (synoptic in winter versus deep convective in summer). The importance of synoptic-scale interactions has been recently highlighted over the Gulf Stream, where the SST gradient is important for storm development, by the thermal damping and strengthening mechanism (Parfitt et al. 2016). This mechanism could be observed in the Agulhas Return Current, where the current and the Southern Hemisphere storm track align (Hoskins and Hodges 2005), or where changes in extratropical storms track and intensity result from smoothing out the Agulhas Current (Reason 2001). Although with a different seasonality (compared to the Gulf Stream), a similar interplay of synoptic versus convective processes could explain the seasonal variations in the dynamic and thermodynamic influence identified in the Agulhas Return Current. However, further work is required to understand how synoptic-scale interactions influence precipitation in the Agulhas Current region of southeast Africa.

In the second part of our study we have identified a mechanism for the influence of the Agulhas Current SST on continental rainfall, through the analysis of geopotential heights and moisture fluxes. In summer and autumn, the Agulhas Current creates a low pressure anomaly above the ocean extending to the land, weakening the anticyclonic motion of the Indian Ocean high pressure system. This favors an influx of moisture from the Agulhas Current to the coast that can go above the escarpment farther inland, thereby enhancing rainfall in South Africa, contributing to even more cyclonic anomalies and leading to further cyclonic moisture transport, in line with Reason and Mulenga (1999) and Reason (2001). The low pressure anomaly is consistent with the solution of shallow atmospheric heating in midlatitudes, with the diabatic heating being balanced by advection of cold air from the south (Hoskins and Karoly 1981). Thus, the low pressure anomaly and cyclonic circulation are positioned eastward of the diabatic heating (i.e., the rainfall maximum is on the western side). The low pressure anomaly could be associated with a baroclinic Rossby wave but further work will be needed to assert that hypothesis. However, at 700 and 500 hPa, the geopotential anomaly is shifted inland westward as would be expected from westward propagation of a Rossby waves (Holton and Hakim 2012). These cyclonic circulation anomalies together with greater moisture availability associated with the 1.5°C warmer SST of the CTL run lead to more moisture flux and therefore to more precipitation over southern Africa. Through this mechanism the Agulhas Current plays an important role in enhancing precipitation over the interior of southern Africa in summer, autumn, and, to lesser extent, spring (Fig. 8b). During winter, the low pressure anomaly does not appear over land, and the supply of moisture flux from the Agulhas is almost nonexistent. The seasonal variations in this mechanism are only partly consistent with the seasonal variations in rainfall over the Agulhas Current (i.e., the diabatic heating is weak in winter, but it is weaker in spring).

Tables 1 and 2 summarize the different mechanisms by which the Agulhas Current SST influences precipitation. Above the Agulhas Current and along the southeastern African coast, the pressure adjustment mechanism contributes to the enhancement of summer and spring precipitation. Spring has less rainfall and so the mechanism is less effective. Winter precipitation is related to the LHF. Inland, the Agulhas Current enhances the summer and autumn precipitation through the influence of strong shallow heating on the lower atmospheric circulation and possibly Rossby wave dynamics. This mechanism is weaker in spring, therefore leading to weaker precipitation enhancement. There is no enhancement of rain in winter, as these mechanisms are not activated.

While the WRF Model used here provides a reasonable simulation of precipitation in the region and we are confident in our results, different results could be found with different models. Here we list several potential issues. The impact of the Agulhas Current on southern African precipitation might be overestimated while the impact over the ocean could be underestimated, as WRF overestimates the land precipitation and underestimates maritime precipitation. Moreover, the uncertainties linked to relative roles of dynamics and thermodynamics in seasonality of the Agulhas Current could be underestimated, as the current is not well represented in the atmospheric model, and its resolution remains relatively low. In particular, the study of Parfitt et al. (2017) highlights the importance of high-resolution SST in resolving the influence of oceanic fronts on weather and climate. In addition, an underestimated influence on maritime rainfall could also affect continental rainfall via the propagation of the Rossby waves. Furthermore, by choosing a southern limit of 43°S and a northern limit of 17°S, some meteorological features that directly impact South African weather and climate could not be properly resolved [e.g., large cold fronts tracking over the Agulhas Current and coast, ridging anticyclones (Weldon and Reason 2014; Engelbrecht et al. 2015; Barimalala et al. 2020), tropical convergence zones (Desbiolles et al. 2018), south Indian Ocean easterly trade winds and the effect of Madagascar (Barimalala et al. 2018), and cutoff lows (Singleton and Reason 2007)]. Also, our model domain is chosen to exclude interactions with remote regions and therefore may overestimate the response of the Agulhas Current on local climate. Therefore, the sensitivity of our results to the model domain should be checked in future studies. Moreover, it could be interesting to perform similar experiments with a global climate model to assess how interactions

with more remote regions could modify the direct local response, following the pioneering work of Reason (2001).

We have shown a definitive seasonal influence of the core of the Agulhas Current on southern Africa precipitation. This has implications for predictability and climate change studies. It argues that high-resolution models with high-resolution SST and realistic latent heat fluxes are needed. We hope the present work will inspire further research on investigating the impacts of the Agulhas Current on climate.

Acknowledgments. Computing resources were provided by NoTur (nn9039k and ns9039k). The authors express their gratitude to the University of Cape Town, the National Research Foundation SARCHi chair on Ocean-Atmosphere Modeling, WRC, ACCESS, DAAD South Africa, the Nansen Tutu Centre for Marine Environmental Research, and the Research Council of Norway funded SANCOOP SCAMPI (234205) and INPART PECO2 (309457) projects for supporting this study. NK and SK are supported by the ERC (Grant 648982) and EU H2020 TRIATLAS projects (Grant 817578). Thanks to Dr. Rodrigue Anicet Imbol Koungue at GEOMAR Helmholtz Centre for Ocean Research Kiel for fruitful discussion on this study.

Data availability statement. The data used for this work are publicly available at the following links: https://rda.ucar.edu/, https://www.ecmwf.int/en/forecasts/datasets/reanalysis-datasets/era5, http://kage.ldeo.columbia.edu/data/TRMM_PR/V2/V1/MonthlyClimatology/, and https://www.ncdc.noaa.gov/oisst/ for CFSR, ERA5, TRMM-PR, and OISST, respectively.

REFERENCES

Barimalala, R., F. Desbiolles, R. C. Blamey, and C. Reason, 2018: Madagascar influence on the south Indian Ocean convergence zone, the Mozambique channel trough and southern African rainfall. *Geophys. Res. Lett.*, **45**, 11 380–11 389, https://doi.org/10.1029/2018GL079964.

——, R. C. Blamey, F. Desbiolles, and C. J. Reason, 2020: Variability in the Mozambique Channel trough and impacts on southeast African rainfall. *J. Climate*, **33**, 749–765, https://doi.org/10.1175/JCLI-D-19-0267.1.

Biasutti, M., S. E. Yuter, C. D. Burleyson, and A. H. Sobel, 2012: Very high-resolution rainfall patterns measured by TRMM precipitation radar: Seasonal and diurnal cycles. *Climate Dyn.*, **39**, 239–258, https://doi.org/10.1007/s00382-011-1146-6.

Blamey, R. C., and C. J. C. Reason, 2013: The role of mesoscale convective complexes in southern Africa summer rainfall. *J. Climate*, **26**, 1654–1668, https://doi.org/10.1175/JCLI-D-12-00239.1.

Cook, C., C. J. C. Reason, and B. C. Hewitson, 2004: Wet and dry spells within particularly wet and dry summers in the South African summer rainfall region. *Climate Res.*, **26**, 17–31, https://doi.org/10.3354/cr026017.

Cook, K. H., 2000: The South Indian convergence zone and interannual rainfall variability over southern Africa. *J. Climate*, **13**, 3789–3804, https://doi.org/10.1175/1520-0442(2000)013<3789:TSICZA>2.0.CO;2.

Crespo, L. R., N. Keenlyside, and S. Koseki, 2018: The role of sea surface temperature in the atmospheric seasonal cycle of the equatorial Atlantic. *Climate Dyn.*, **52**, 5927–5946, https://doi.org/10.1007/s00382-018-4489-4.

Crétat, J., B. Pohl, B. Dieppois, S. Berthou, and J. Pergaud, 2019: The Angola low: Relationship with southern African rainfall and ENSO. *Climate Dyn.*, **52**, 1783–1803, https://doi.org/10.1007/s00382-018-4222-3.

D'Abreton, P. C., and J. A. Lindesay, 1993: Water vapour transport over southern Africa during wet and dry early and late summer months. *Int. J. Climatol.*, **13**, 151–170, https://doi.org/10.1002/joc.3370130203.

Dee, D. P., and Coauthors, 2011: The ERA-Interim reanalysis: Configuration and performance of the data assimilation system. *Quart. J. Roy. Meteor. Soc.*, **137**, 553–597, https://doi.org/10.1002/qj.828.

Desbiolles, F., R. Blamey, S. Illig, R. James, R. Barimalala, L. Renault, and C. Reason, 2018: Upscaling impact of wind/sea surface temperature mesoscale interactions on southern Africa austral summer climate. *Int. J. Climatol.*, **38**, 4651–4660, https://doi.org/10.1002/joc.5726.

——, E. Howard, R. C. Blamey, R. Barimalala, N. C. Hart, and C. J. Reason, 2020: Role of ocean mesoscale structures in shaping the Angola-Low pressure system and the southern Africa rainfall. *Climate Dyn.*, **54**, 3685–3704, https://doi.org/10.1007/s00382-020-05199-1.

Dieppois, B., B. Pohl, M. Rouault, M. New, D. Lawler, and N. Keenlyside, 2016: Interannual to interdecadal variability of winter and summer southern African rainfall, and their teleconnections. *J. Geophys. Res. Atmos.*, **121**, 6215–6239, https://doi.org/10.1002/2015JD024576.

Driver, P., and C. J. C. Reason, 2017: Variability in the Botswana High and its relationships with rainfall and temperature characteristics over southern Africa. *Int. J. Climatol.*, **37** (Suppl. 1), 570–581, https://doi.org/10.1002/joc.5022.

Engelbrecht, C. J., and W. A. Landman, 2016: Interannual variability of seasonal rainfall over the Cape south coast of South Africa and synoptic type association. *Climate Dyn.*, **47**, 295–313, https://doi.org/10.1007/s00382-015-2836-2.

——, ——, F. A. Engelbrecht, and J. Malherbe, 2015: A synoptic decomposition of rainfall over the Cape south coast of South Africa. *Climate Dyn.*, **44**, 2589–2607, https://doi.org/10.1007/s00382-014-2230-5.

Favre, A., B. Hewitson, C. Lennard, R. Cerezo-Mota, and M. Tadross, 2013: Cut-off lows in the South Africa region and their contribution to precipitation. *Climate Dyn.*, **41**, 2331–2351, https://doi.org/10.1007/s00382-012-1579-6.

——, and Coauthors, 2016: Spatial distribution of precipitation annual cycles over South Africa in 10 CORDEX regional climate model present-day simulations. *Climate Dyn.*, **46**, 1799–1818, https://doi.org/10.1007/s00382-015-2677-z.

Hart, N. C., C. J. C. Reason, and N. Fauchereau, 2013: Cloud bands over southern Africa: Seasonality, contribution to rainfall variability and modulation by the MJO. *Climate Dyn.*, **41**, 1199–1212, https://doi.org/10.1007/s00382-012-1589-4.

Hersbach, H., and Coauthors, 2020: The ERA5 global reanalysis. *Quart. J. Roy. Meteor. Soc.*, **146**, 1999–2049, https://doi.org/10.1002/qj.3803.

Hewitson, B. C., and R. G. Crane, 2005: Gridded area-averaged daily precipitation via conditional interpolation. *J. Climate*, **18**, 41–57, https://doi.org/10.1175/JCLI3246.1.

Holton, J. R., and G. J. Hakim, 2012: *An Introduction to Dynamic Meteorology*. Academic Press, 171–210.

Hoskins, B. J., and D. Karoly, 1981: The steady linear response of a spherical atmosphere to thermal and orographic forcing. *J. Atmos. Sci.*, **38**, 1179–1196, https://doi.org/10.1175/1520-0469(1981)038<1179:TSLROA>2.0.CO;2.

——, and K. I. Hodges, 2005: A new perspective on Southern Hemisphere storm tracks. *J. Climate*, **18**, 4108–4129, https://doi.org/10.1175/JCLI3570.1.

Hutchinson, K., L. M. Beal, P. Penven, I. Ansorge, and J. Hermes, 2018: Seasonal phasing of Agulhas Current transport tied to a baroclinic adjustment of near-field winds. *J. Geophys. Res. Oceans*, **123**, 7067–7083, https://doi.org/10.1029/2018JC014319.

Imbol Nkwinkwa, A. S., M. Rouault, and J. A. Johannessen, 2019: Latent heat flux in the Agulhas Current. *Remote Sens.*, **11**, 1576, https://doi.org/10.3390/rs11131576.

Jury, M. R., 2015: Passive suppression of South African rainfall by the Agulhas Current. *Earth Interact.*, **19**, https://doi.org/10.1175/EI-D-15-0017.1.

——, H. R. Valentine, and J. R. Lutjeharms, 1993: Influence of the Agulhas Current on summer rainfall along the southeast coast of South Africa. *J. Appl. Meteor. Climatol.*, **32**, 1282–1287, https://doi.org/10.1175/1520-0450(1993)032<1282:IOTACO>2.0.CO;2.

——, B. Pathack, C. D. W. Rautenbach, and J. Vanheerden, 1997: Drought over South Africa and Indian Ocean SST: Statistical and GCM results. *Global Ocean Atmos. Syst.*, **4**, 47–63.

Koseki, S., and T. Demissie, 2018: Does the Drakensberg dehydrate southwestern Africa? *J. Arid Environ.*, **158**, 35–42, https://doi.org/10.1016/j.jaridenv.2018.08.003.

——, B. Pohl, B. C. Bhatt, N. Keenlyside, and A. S. Nkwinkwa Njouodo, 2018: Insights into the summer diurnal cycle over eastern South Africa. *Mon. Wea. Rev.*, **146**, 4339–4356, https://doi.org/10.1175/MWR-D-18-0184.1.

Krug, M., and J. Tournadre, 2012: Satellite observations of an annual cycle in the Agulhas Current. *Geophys. Res. Lett.*, **39**, https://doi.org/10.1029/2012GL052335.

——, D. Schilperoort, F. Collard, M. W. Hansen, and M. Rouault, 2018: Signature of the Agulhas Current in high resolution satellite derived wind fields. *Remote Sens. Environ.*, **217**, 340–351, https://doi.org/10.1016/j.rse.2018.08.016.

Kushnir, Y., W. A. Robinson, I. Blade, N. M. J. Hall, S. Peng, and R. Sutton, 2002: Atmospheric GCM response to extratropical SST anomalies: Synthesis and evaluation. *J. Climate*, **15**, 2233–2256, https://doi.org/10.1175/1520-0442(2002)015<2233:AGRTES>2.0.CO;2.

Lee-Thorp, A. M., M. Rouault, and J. R. E. Lutjeharms, 1999: Moisture uptake in the boundary layer above the Agulhas Current: A case study. *J. Geophys. Res.*, **104**, 1423–1430, https://doi.org/10.1029/98JC02375.

Lindzen, R. S., and S. Nigam, 1987: On the role of sea surface temperature gradients in forcing low-level winds and convergence in the tropics. *J. Atmos. Sci.*, **44**, 2418–2436, https://doi.org/10.1175/1520-0469(1987)044<2418:OTROSS>2.0.CO;2.

Macron, C., B. Pohl, Y. Richard, and M. Bessafi, 2014: How do tropical temperate troughs form and develop over southern Africa? *J. Climate*, **27**, 1633–1647, https://doi.org/10.1175/JCLI-D-13-00175.1.

Malherbe, J., F. A. Engelbrecht, W. A. Landman, and C. J. Engelbrecht, 2012: Tropical systems from the southwest Indian Ocean making landfall over the Limpopo River Basin, southern Africa: A historical perspective. *Int. J. Climatol.*, **32**, 1018–1032, https://doi.org/10.1002/joc.2320.

Minobe, S., A. Kuwano-Yoshida, N. Komori, S.-P. Xie, and R. J. Small, 2008: Influence of the Gulf Stream on the troposphere. *Nature*, **452**, 206–209, https://doi.org/10.1038/nature06690.

——, M. Miyashita, A. Kuwano-Yoshida, H. Tokinaga, and S.-P. Xie, 2010: Atmospheric response to the Gulf Stream: Seasonal variations. *J. Climate*, **23**, 3699–3719, https://doi.org/10.1175/2010JCLI3359.1.

Monerie, P.-A., J. Robson, B. Dong, B. Dieppois, B. Pohl, and N. Dunstone, 2018: Predicting the seasonal evolution of southern African summer precipitation in the DePreSys3 prediction system. *Climate Dyn.*, **52**, 6491–6510, https://doi.org/10.1007/s00382-018-4526-3.

Nikulin, G., and Coauthors, 2012: Precipitation climatology in an ensemble of COREDEX-Africa regional climate simulations. *J. Climate*, **25**, 6057–6078, https://doi.org/10.1175/JCLI-D-11-00375.1.

Nkwinkwa Njouodo, A. S., 2018: On the role of the Agulhas Current on weather and climate of South Africa. Doctoral thesis, Dept. of Oceanography, University of Cape Town, 170 pp.

——, S. Koseki, N. Keenlyside, and M. Rouault, 2018: Atmospheric signature of the Agulhas Current. *Geophys. Res. Lett.*, **45**, 5185–5193, https://doi.org/10.1029/2018GL077042.

O'Neill, L. W., T. Haack, D. B. Chelton, and E. Skyllingstad, 2017: The Gulf Stream convergence zone in the time-mean winds. *J. Atmos. Sci.*, **74**, 2383–2412, https://doi.org/10.1175/JAS-D-16-0213.1.

Parfitt, R., and A. Czaja, 2016: On the contribution of synoptic transients to the mean atmospheric state in the Gulf Stream region. *Quart. J. Roy. Meteor. Soc.*, **142**, 1554–1561, https://doi.org/10.1002/qj.2689.

——, ——, S. Minobe, and A. Kuwano-Yoshida, 2016: The atmospheric frontal response to SST perturbations in the Gulf Stream region. *Geophys. Res. Lett.*, **43**, 2299–2306, https://doi.org/10.1002/2016GL067723.

——, ——, and Y. O. Kwon, 2017: The impact of SST resolution change in the ERA-Interim reanalysis on wintertime Gulf Stream frontal air–sea interaction. *Geophys. Res. Lett.*, **44**, 3246–3254, https://doi.org/10.1002/2017GL073028.

Pohl, B., M. Rouault, and S. S. Roy, 2014: Simulation of the annual and diurnal cycles of rainfall over South Africa by a regional climate model. *Climate Dyn.*, **43**, 2207–2226, https://doi.org/10.1007/s00382-013-2046-8.

Reason, C. J. C., 2001: Evidence for the influence of the Agulhas Current on regional atmospheric circulation patterns. *J. Climate*, **14**, 2769–2778, https://doi.org/10.1175/1520-0442(2001)014<2769:EFTIOT>2.0.CO;2.

——, 2017. Climate of southern Africa. *Oxford Research Encyclopedia of Climate Science*, https://doi.org/10.1093/acrefore/9780190228620.013.513.

——, and H. Mulenga, 1999: Relationships between South African rainfall and SST anomalies in the southwest Indian Ocean. *Int. J. Climatol.* **19**, 1651–1673, https://doi.org/10.1002/(SICI)1097-0088(199912)19:15<1651::AID-JOC439>3.0.CO;2-U.

——, W. Landman, and W. Tennant, 2006: Seasonal to decadal prediction of southern African climate and its links with variability of the Atlantic Ocean. *Bull. Amer. Meteor. Soc.*, **87**, 941–956, https://doi.org/10.1175/BAMS-87-7-941.

Reynolds, R. W., T. M. Smith, C. Liu, D. B. Chelton, K. S. Casey, and M. G. Schlax, 2007: Daily high-resolution-blended analyses for sea surface temperature. *J. Climate*, **20**, 5473–5496, https://doi.org/10.1175/2007JCLI1824.1.

Rouault, M., and J. R. E. Lutjeharms, 2000: Air–sea exchange over an Agulhas eddy at the subtropical convergence. *Global Atmos. Ocean Syst.*, **7**, 125–150.

——, and ——, 2003: Estimation of sea-surface temperature around southern Africa from satellite-derived microwave observations. *S. Afr. J. Sci.*, **99**, 489–494.

——, A. M. Lee-Thorp, and J. R. E. Lutjeharms, 2000: The atmospheric boundary layer above the Agulhas Current during alongcurrent winds. *J. Phys. Oceanogr.*, **30**, 40–50, https://doi.org/10.1175/1520-0485(2000)030<0040:TABLAT>2.0.CO;2.

——, C. J. C. Reason, J. R. E. Lutjeharms, and A. C. M. Beljaars, 2003: Underestimation of latent and sensible heat fluxes above the Agulhas Current in NCEP and ECMWF analyses. *J. Climate*, **16**, 776–782, https://doi.org/10.1175/1520-0442(2003)016<0776:UOLASH>2.0.CO;2.

——, S. S. Roy, and R. C. Balling, 2013: The diurnal cycle of rainfall in South Africa in the austral summer. *Int. J. Climatol.*, **33**, 770–777, https://doi.org/10.1002/joc.3451.

Saha, S., and Coauthors, 2010: The NCEP Climate Forecast System Reanalysis. *Bull. Amer. Meteor. Soc.*, **91**, 1015–1058, https://doi.org/10.1175/2010BAMS3001.1.

Singleton, A. T., and C. J. C. Reason, 2007: Variability in the characteristics of cut-off low pressure systems over subtropical southern Africa. *Int. J. Climatol.* **27**, 295–310, https://doi.org/10.1002/joc.1399.

Skamarock, W. C., and J. B. Klemp, 2008: A time-split nonhydrostatic atmospheric model for weather research and forecasting applications. *J. Comput. Phys.*, **227**, 3465–3485, https://doi.org/10.1016/j.jcp.2007.01.037.

Sutton, R., and P. P. Mathieu, 2002: Response of the atmosphere–ocean mixed-layer system to anomalous ocean heat-flux convergence. *Quart. J. Roy. Meteor. Soc.*, **128**, 1259–1275, https://doi.org/10.1256/003590002320373283.

Takatama, K., S. Minobe M. Inatsu, and R. J. Small, 2012: Diagnostics for near-surface wind convergence/divergence response to the Gulf Stream in a regional atmospheric model. *Atmos. Sci. Lett.*, **13**, 16–21, https://doi.org/10.1002/asl.355.

Tyson, D., and R. A. Preston-White, 2000: *The Weather and Climate of Southern Africa*. Oxford University Press, 396 pp.

Vigaud, N., Y. Richard, M. Rouault, and N. Fauchereau, 2007: Water vapour transport from the tropical Atlantic and summer rainfall in tropical southern Africa. *Climate Dyn.*, **28**, 113–123, https://doi.org/10.1007/s00382-006-0186-9.

——, ——, ——, and ——, 2009: Moisture transport between the South Atlantic Ocean and southern Africa: Relationships with summer rainfall and associated dynamics. *Climate Dyn.*, **32**, 113–123, https://doi.org/10.1007/s00382-008-0377-7.

——, B. Pohl, and J. Crétat, 2012: Tropical–temperate interactions over southern Africa simulated by a regional climate model. *Climate Dyn.*, **39**, 2895–2916, https://doi.org/10.1007/s00382-012-1314-3.

Weldon, D., and C. J. C. Reason, 2014: Variability of rainfall characteristics over the South Coast region of South Africa. *Theor. Appl. Climatol.*, **115**, 177–185, https://doi.org/10.1007/s00704-013-0882-4.